Electronic Supplementary Information for

# Insights into the Unusual Semiconducting Behavior in Low-Dimensional Boron

Shao-Gang Xu,[‡a, b, c] Xiao-Tian Li,[‡b] Yu-Jun Zhao,[b] Wang-Ping Xu,[a] Ji-Hai Liao,[b,d] Xiu-Wen Zhang,[c] Hu Xu[*a] and Xiao-Bao Yang[*b]

[a]*Department of Physics and Shenzhen Key Laboratory of Quantum Science and Engineering, Southern University of Science and Technology, Shenzhen 518055, P. R. China*

[b]*Department of Physics, South China University of Technology, Guangzhou 510640, P. R. China*

[c]*College of Electronic Science and Technology, Shenzhen University, Shenzhen 518060, P. R. China*

[d]*State Key Laboratory of Metastable Materials Science and Technology ,Yanshan University, Qinhuangdao 066004,China*

[*]Corresponding author Email: xuh@sustc.edu.cn; scxbyang@scut.edu.cn

## Average Formation Energy:

The average formation energy ($E_{\text{form}}$) of the B sandwiches is defined as $E_{\text{form}} = (E_{\text{tot}}/n - E_{\text{at}})$, where $E_{\text{tot}}$ is the total energy of the B sandwiches, $E_{\text{at}}$ is the energy of an isolated spin-polarized boron atom, and $n$ is the number of B atoms in the cell.

## Thermodynamic Phase Diagram:

In order to further examine the stability of different 2D B allotropes deposited on metal substrates, we define the average formation energy($E_{\text{form}}$) as

$$E_{form} = \frac{1}{A}\left(E_{tot} - E_{sub} - n \times \mu_B\right)$$

where the $E_{\text{tot}}$, $E_{\text{sub}}$ represent the total energy of the B/metal systems and the metal substrates respectively, $n$ is the number of B atoms of the absorbed 2D boron allotropes, $A$ is the area of the 2D boron structures, and $\mu_B$ is the chemical potential of B atoms. Under the B-rich condition, $\mu_B$ is referred to the per atom energy of α phase $\mu_{B(crystal)}$. Based on the above equation, the formation energies of various 2D boron structures on metal substrates as a function of B chemical potential ($\Delta\mu_B = \mu_B - \mu_{B(crystal)}$) can be obtained. The atomic structures of the 2D boron allotropes growth on

the metal substrates are shown in Fig. S13. Note that, we modeled the substrate using the five-layer slab with the bottom two layers fixed, considering a few possible configurations of 2D boron allotropes on the substrates where the absolute value of lattice mismatch δ is under 2.5%.

## Power Conversion Efficiency:

The power conversion efficiency (PCE) $\eta$ is estimated in the limit of 100% external quantum efficiency (EQE)[1,2] described as

$$\eta = \frac{J_{sc} V_{oc} \beta_{FF}}{P_{solar}} = \frac{0.65\left(E_g^d - \Delta E_c - 0.3\right)\int_{E_g}^{\infty} \frac{P(\hbar\varpi)}{\hbar\varpi} d(\hbar\varpi)}{\int_0^{\infty} P(\hbar\varpi) d(\hbar\varpi)}$$

where 0.65 is the band-fill factor ($\beta_{FF}$), $P(\hbar\varpi)$ is the AM1.5 solar energy flux(expressed in W/m$^{-2}$/eV$^{-1}$) at the photo energy $(\hbar\varpi)$, and $E_g^d$ is the bandgap of the donor, and $\Delta E_c$ represents the conduction band (CB) offset between donor and acceptor, and the $\left(E_g^d - \Delta E_c - 0.3\right)$ term is an estimation of the maximum open circuit voltage $V_{oc}$ (here in eV units). The integral in the numerator is the short circuit current $J_{sc}$ performed applying the limit EQE of 100%, and the integral in the denominator is the incident solar radiation (AM1.5 solar flux).

## Number of Electrons:

We have calculated the projected density of states (PDOS) for the 2D boron allotropes, and the number($N$) of electrons of the ($s$, $p_x$, $p_y$ and $p_z$) orbitals for the given B atom is defined as

$$N = \int_{-\infty}^{E_F} D(E) d(E)$$

where $E_F$ represents the Fermi level of the system, and D($E$) is the PDOS value for the given B atoms.

**REFERENCES**:

(1) Bernardi, M.; Palummo, M.; Grossman, J. C., *ACS Nano* 2012, **6**, 10082-10089;
(2) Scharber, M. C.; Mühlbacher, D.; Koppe, M.; Denk, P.; Waldauf, C.; Heeger, A. J.; Brabec, C. J., *Adv. Mater.* 2006, **18**, 789-794.

Table S1. The symmetric groups(SG), calculated lattice constants by PBE functional, the band gaps calculated by HSE06 functional, and the average formation energy $E_{form}$ of all the

2D boron allotropes from GGA(PBE) results.

| Phase | SG | *a*(Å) | *b*(Å) | γ(°) | Bandgap(eV)-HSE06 | $E_{form}$(eV/atom)-PBE |
|---|---|---|---|---|---|---|
| $\eta_{1/8}$ | *Pmma*(51) | 5.07 | 11.709 | 90 | | -5.997 |
| *P6/mmm* | *P6/mmm*(191) | 2.865 | 2.865 | 120 | | -6.002 |
| *Pmmn* | *Pmmn*(59) | 4.520 | 3.260 | 90 | | -6.056 |
| *Pmmm* | *Pmmm*(47) | 2.88 | 3.26 | 90 | | -6.082 |
| $\gamma_{28}$-film | *P2/m*(10) | 5.624 | 6.988 | 90 | | -5.896 |
| R1($T_A$) | *P2/m*(10) | 3.332 | 4.408 | 79.11 | 0.305 | -6.043 |
| R2($T_B$) | *P-6m2*(187) | 4.986 | 4.986 | 120 | 1.428 | -6.027 |
| R3 | *Pbam*(55) | 3.333 | 8.659 | 90 | 0.861 | -6.059 |
| R4($T_{AB}$) | *Pm*(6) | 4.992 | 7.253 | 83.41 | 0.975 | -6.020 |
| $T_{AAB}$ | *Pm*(6) | 4.992 | 10.122 | 85.29 | 1.014 | -6.027 |
| $T_{ABB}$ | *Pm*(6) | 4.992 | 11.648 | 81.79 | 1.073 | -6.021 |
| $T_{ABBB}$ | *Pm*(6) | 4.992 | 15.874 | 86.99 | 1.050 | -6.022 |
| $T_{AAAB}$ | *Pm*(6) | 4.992 | 13.208 | 79.11 | 0.822 | -6.031 |
| $T_{ABBA}$ | *Pm*(6) | 4.992 | 14.507 | 83.41 | 0.808 | -6.026 |
| $T_{AAAAB}$ | *Pm*(6) | 4.992 | 15.874 | 86.99 | 0.632 | -6.033 |
| $T_{ABAAB}$ | *Pm*(6) | 4.992 | 17.293 | 90 | 0.994 | -6.024 |
| $T_{AABBA}$ | *Pm*(6) | 4.992 | 17.293 | 90 | 0.541 | -6.028 |

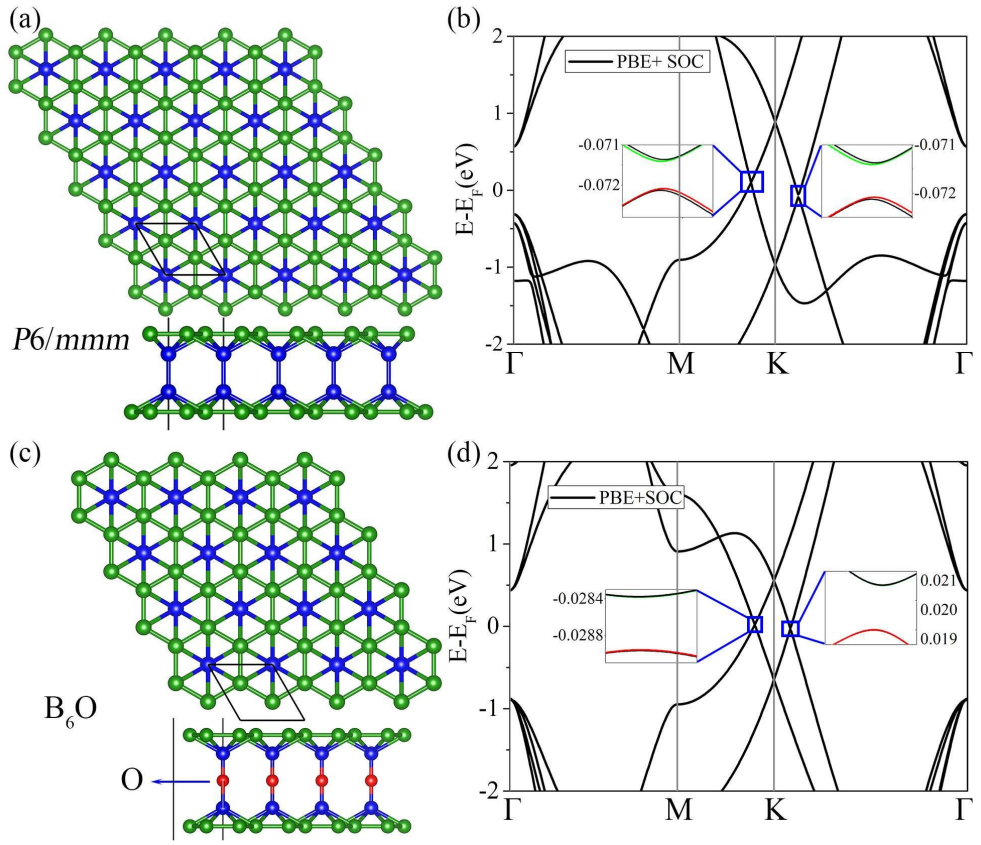


Fig. S1 (a, c) The atomic structures of bilayer *P6/mmm* and $B_6O$ sandwich (top view and side view). (b, d) The PBE band structures of *P6/mmm* and $B_6O$ in the presence of SOC effect.

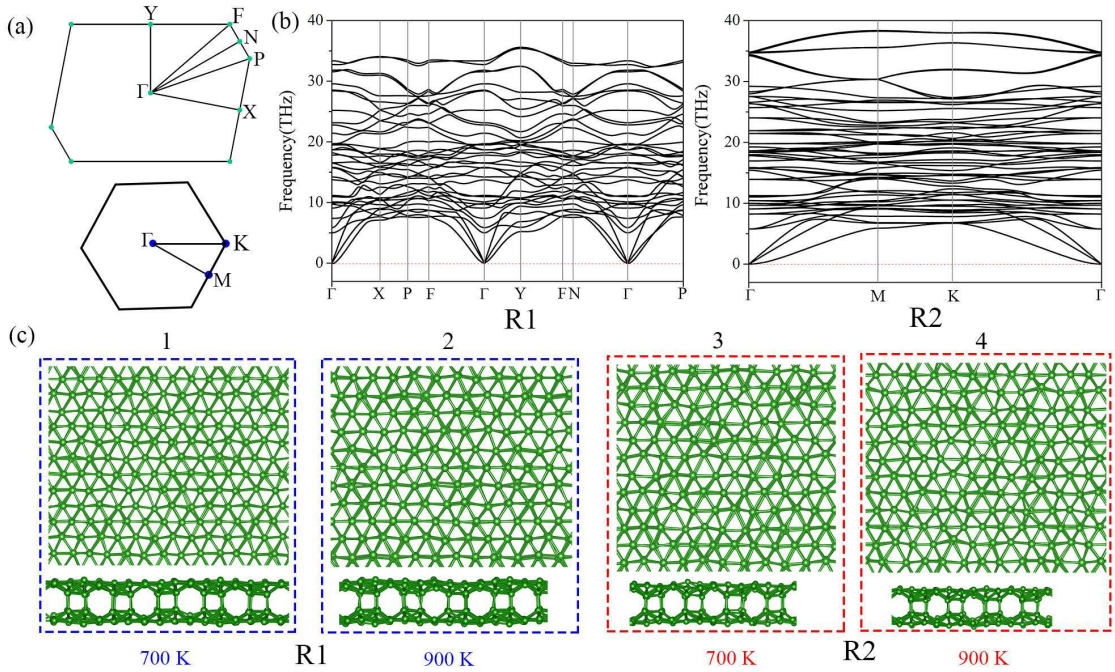


Fig. S2 (a) The first Brillouin zones for R1 and R2. (b) The phonon dispersions along the high-symmetry line of R1 and R2. (c) The AIMD snapshots at the temperature of 700 K/900 K (10 ps) for R1 and R2, respectively.

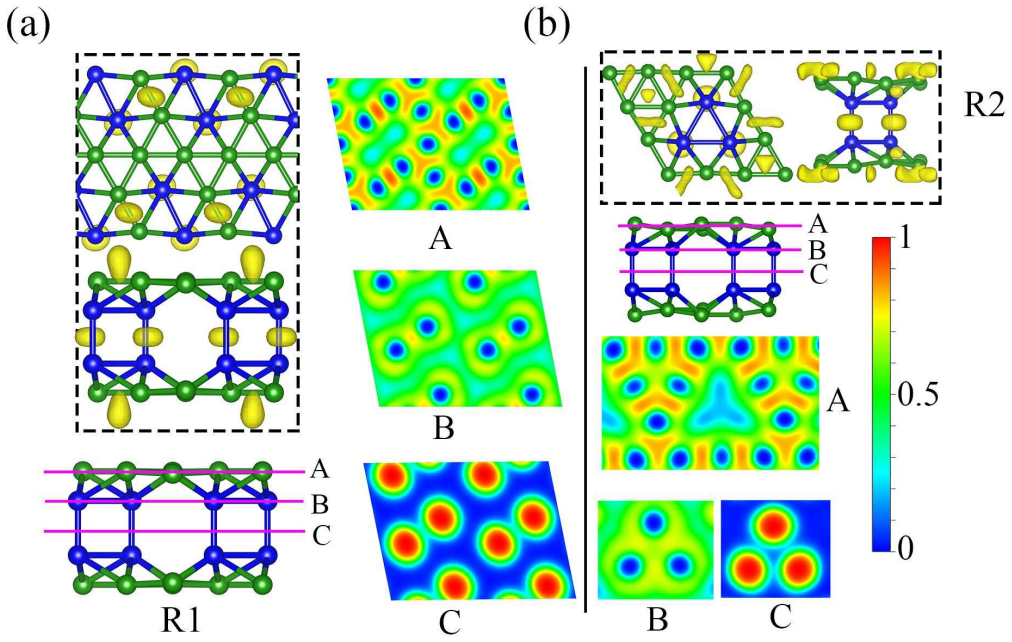


Fig. S3 (a, b) The top view and side view of the electron localization function(ELF) of R1(0.85) and R2(0.82), and A-C display the 2D ELF of R1/R2 sliced planes.

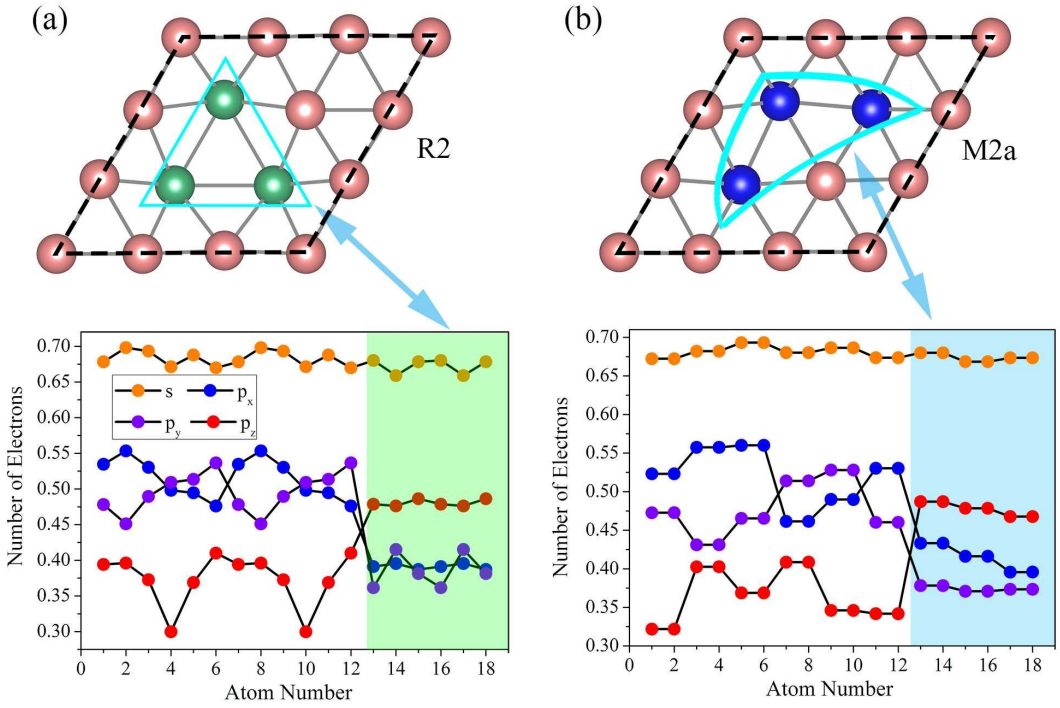


Fig. S4 (a, b) The top view for the 2D boron allotropes(R2, M2a), and the number of electrons of the projected orbitals for the given boron atoms. The green region and the blue region represent the results for the six boron atoms of the interlayer bonds.

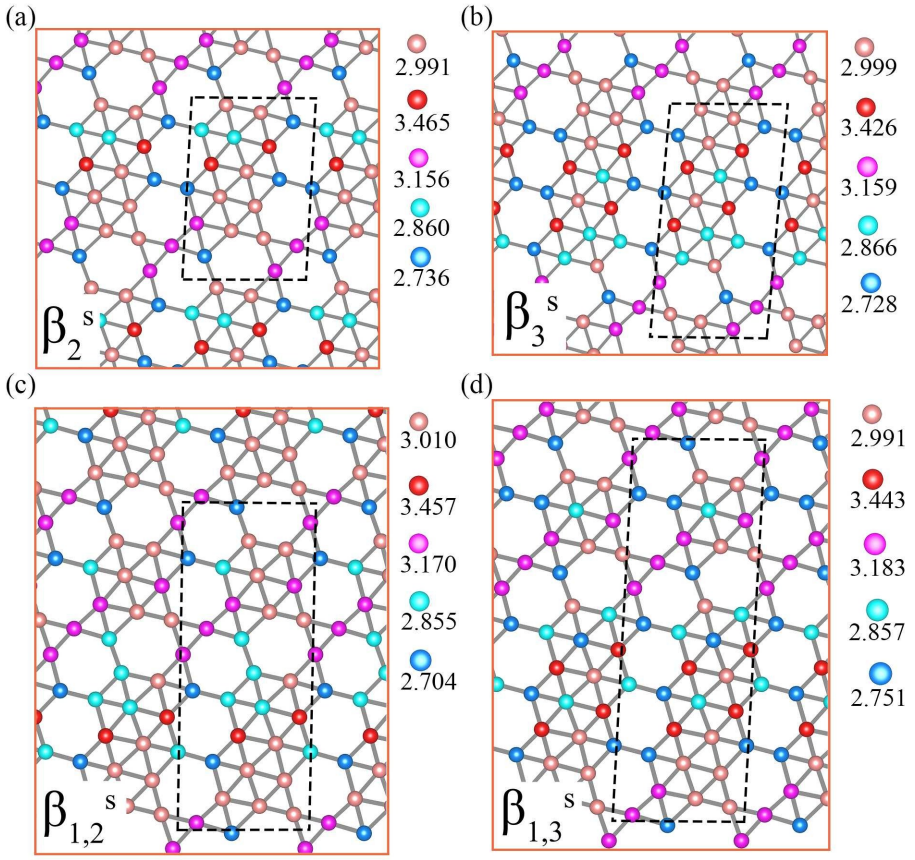


Fig. S5 (a-d) represent Bader charge analysis for the four typical semiconducting boron monolayers, and the values present at the right side are the average value of the given color atoms.

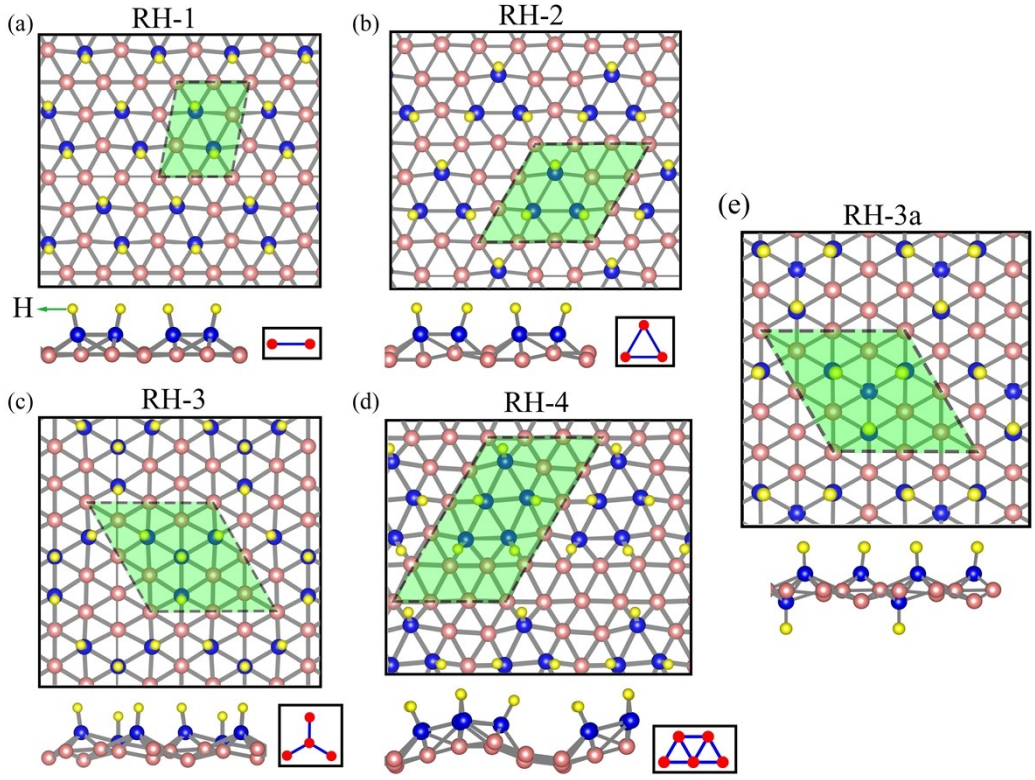

Fig. S6 The atomic configurations of hydrogen adsorption on various triangular boron sheet super-cells. The blue atoms represent the boron atoms at the adsorption sites. The adsorption configurations are shown in the bottom corner of the corresponding structures. The black dash lines represent the unit cells of the corresponding structures.

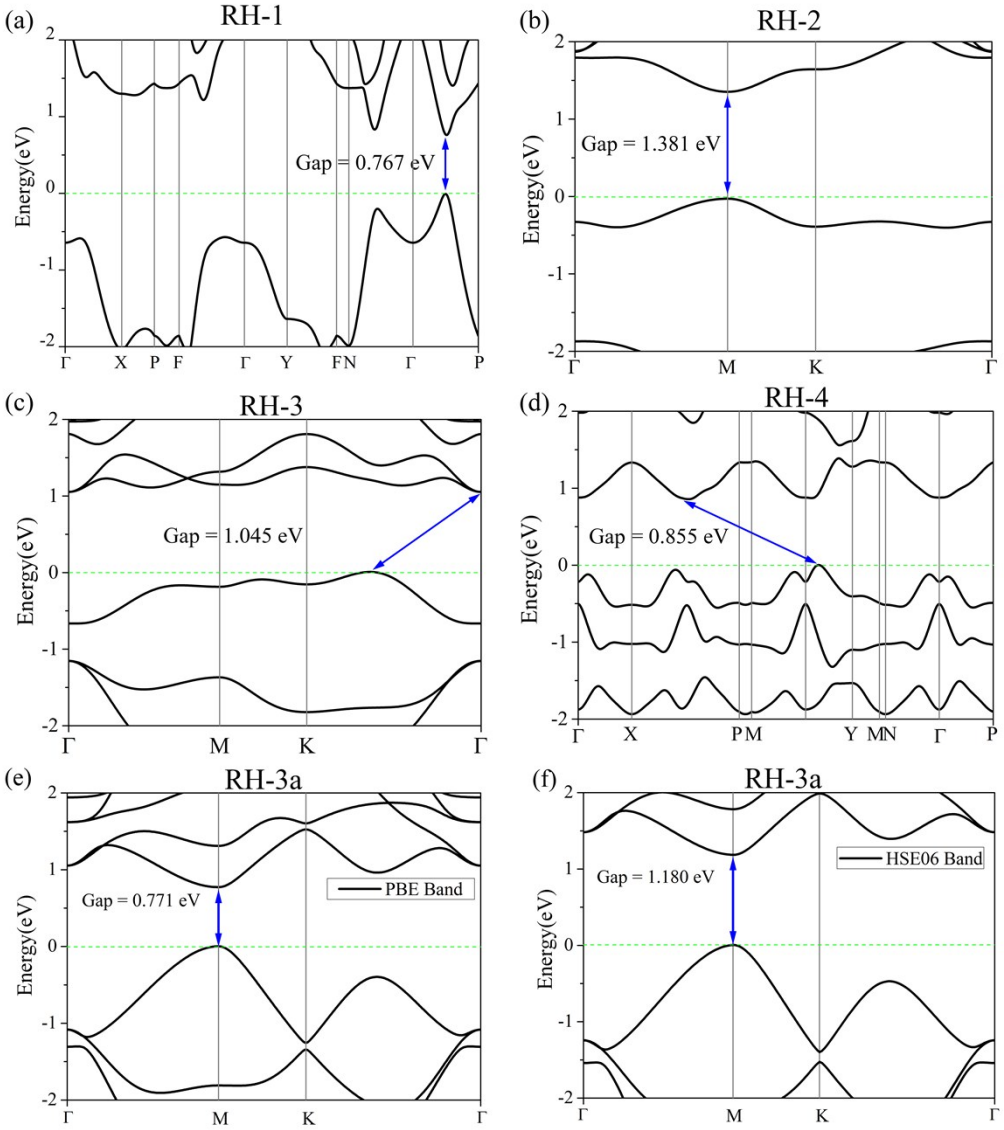


Fig. S7 (a-d) The band structures of the hydrogen adsorption triangular boron sheet super-cells at PBE level. (e, f) The PBE and HSE06 band structures of 2D RH-3a phase. The blue arrows represent the position of the VBM and CBM of the corresponding adsorption systems (VBM is set to 0).

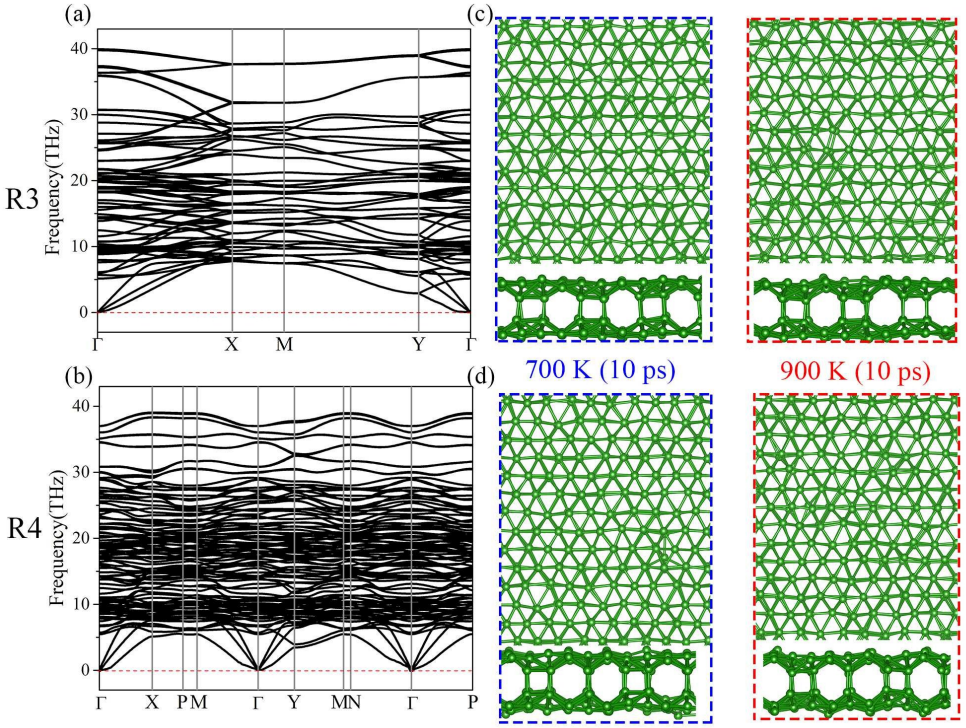


Fig. S8 (a, b) The phonon dispersions along the high-symmetry lines of R3 and R4. (c, d) The AIMD snapshots at the temperature of 700 K/900 K (10 ps) for R3 and R4, respectively.

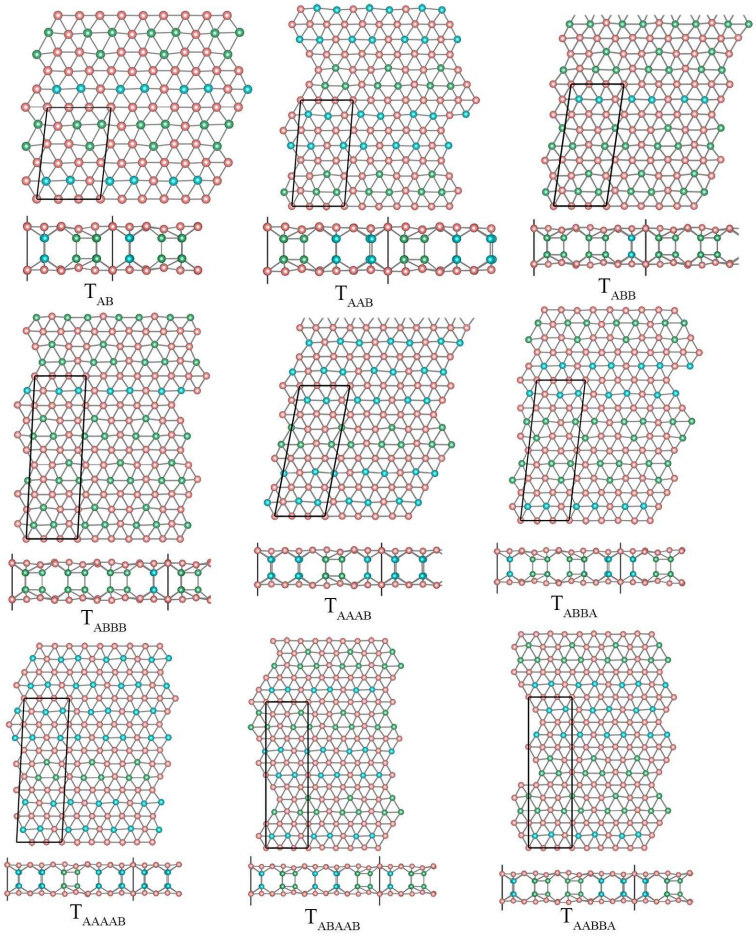

Fig. S9 The atomic structures of the new designed stable boron sandwiches (top view and side view). The black solid lines represent the unit cells of the corresponding structures.

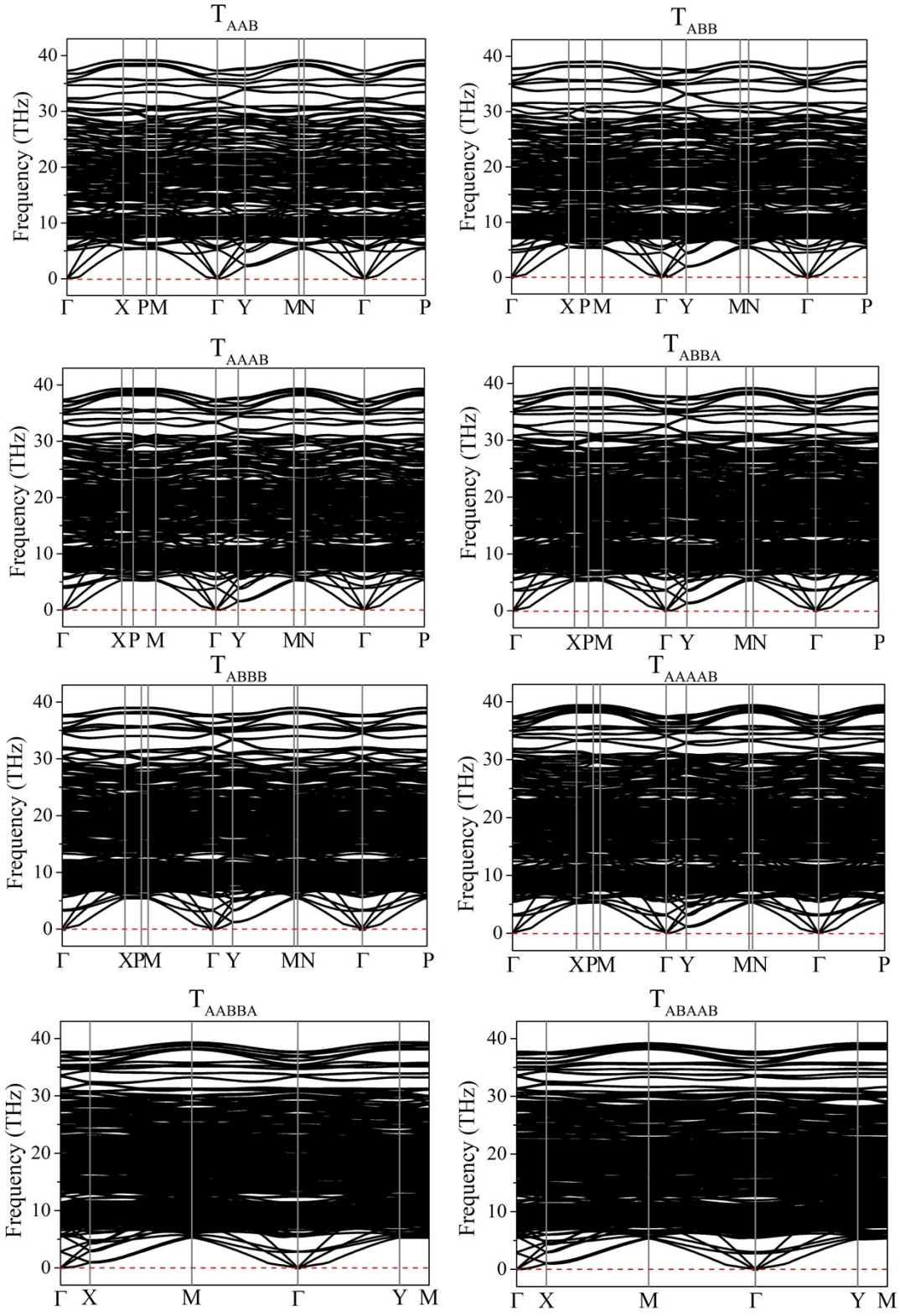


Fig. S10 The phonon dispersions along the high-symmetry lines for the new designed sandwiches.

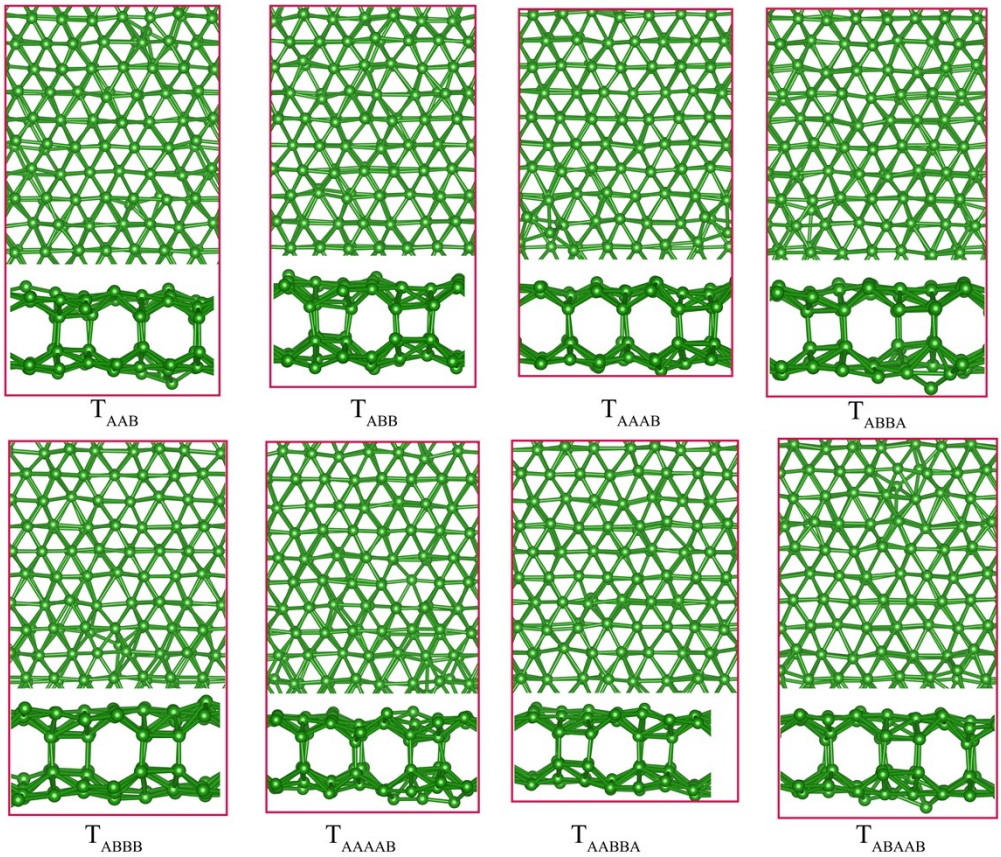


Fig. S11 AIMD snapshots of the atomic structures for the new designed sandwiches at the moment of 10 ps at 700 K (top view and side view).

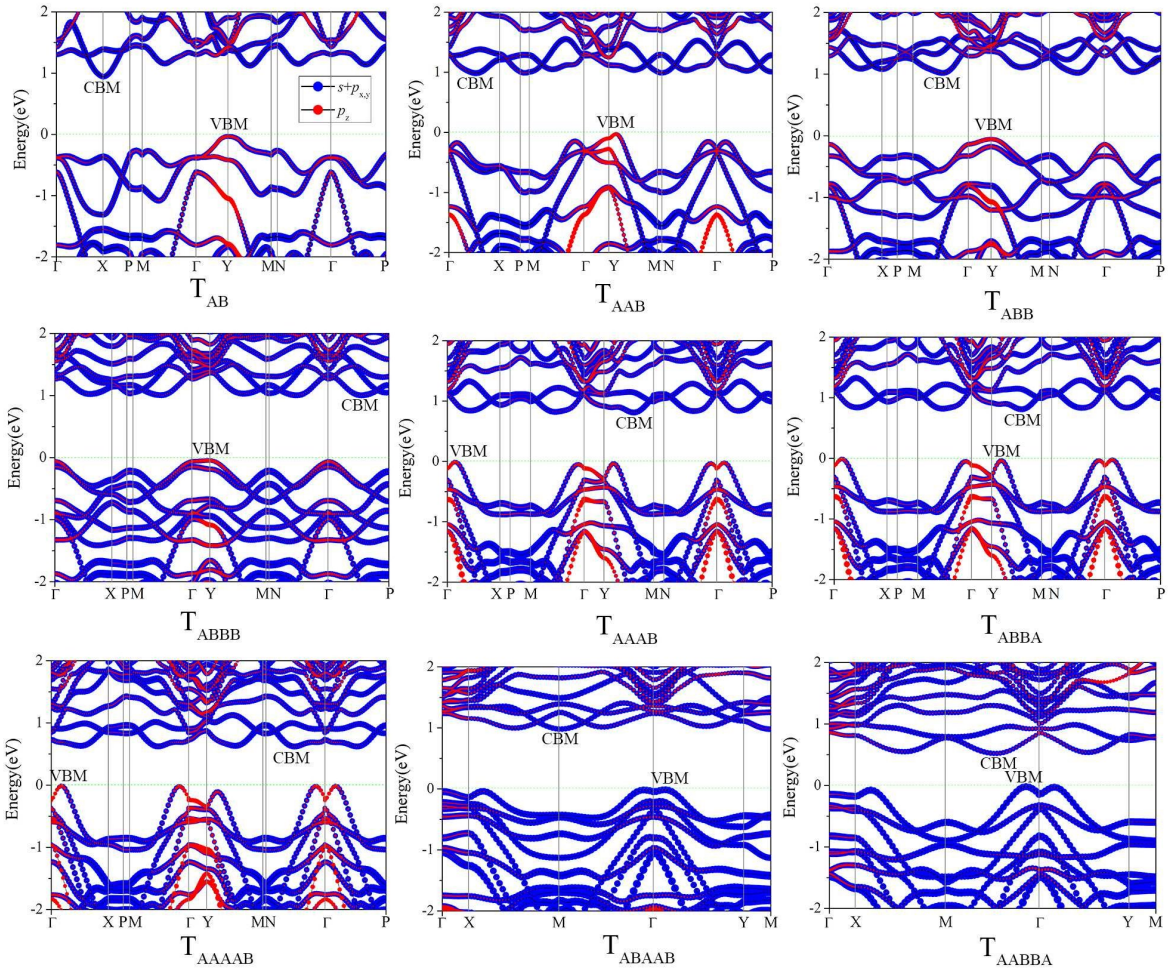


Fig. S12 The projected band structures (HSE06) of the new designed boron sandwiches. (VBM is set to 0.)

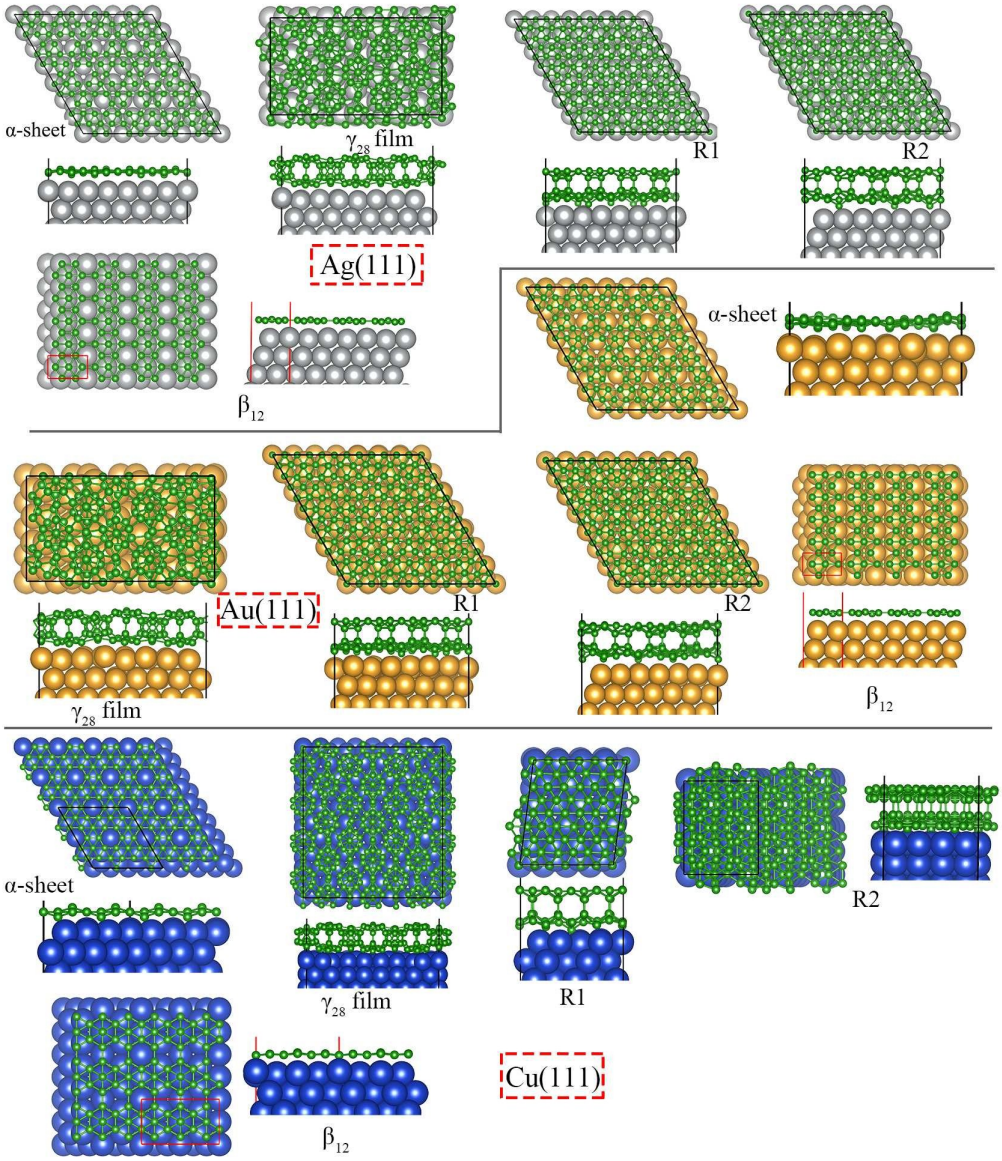


Fig. S13 The atomic structures(top view and side view) of the 2D boron allotropes growth on the metal substrates. The solid lines represent the unit cells of the corresponding absorption systems.